

## Probing plasmonic breathing modes optically

Markus K. Krug, Michael Reisecker, Andreas Hohenau, Harald Dittlbacher, Andreas Trügler, Ulrich Hohenester, and Joachim R. Krenn

Citation: [Applied Physics Letters](#) **105**, 171103 (2014); doi: 10.1063/1.4900615

View online: <http://dx.doi.org/10.1063/1.4900615>

View Table of Contents: <http://scitation.aip.org/content/aip/journal/apl/105/17?ver=pdfcov>

Published by the [AIP Publishing](#)

---

### Articles you may be interested in

[Influence of surface plasmon resonances of silver nanoparticles on optical and electrical properties of textured silicon solar cell](#)

*Appl. Phys. Lett.* **104**, 073903 (2014); 10.1063/1.4866163

[The size and structure of Ag particles responsible for surface plasmon effects and luminescence in Ag homogeneously doped bulk glass](#)

*J. Appl. Phys.* **114**, 073102 (2013); 10.1063/1.4818830

[Localized surface plasmon-enhanced electroluminescence from ZnO-based heterojunction light-emitting diodes](#)

*Appl. Phys. Lett.* **99**, 181116 (2011); 10.1063/1.3658392

[Structure and optical properties of self-assembled multicomponent plasmonic nanogels](#)

*Appl. Phys. Lett.* **99**, 043112 (2011); 10.1063/1.3615785

[Optical spectroscopy and energy-filtered transmission electron microscopy of surface plasmons in core-shell nanoparticles](#)

*J. Appl. Phys.* **101**, 024307 (2007); 10.1063/1.2424404

---

The advertisement features a blue background with a film strip graphic on the left. The text is in white and orange. The Oxford Instruments logo is in the bottom right corner.

**Not all AFMs are created equal**  
**Asylum Research Cypher™ AFMs**  
**There's no other AFM like Cypher**

[www.AsylumResearch.com/NoOtherAFMLikeIt](http://www.AsylumResearch.com/NoOtherAFMLikeIt)

**OXFORD**  
INSTRUMENTS  
*The Business of Science®*

## Probing plasmonic breathing modes optically

Markus K. Krug,<sup>a)</sup> Michael Reisecker, Andreas Hohenau, Harald Dittbacher, Andreas Trügler, Ulrich Hohenester, and Joachim R. Krenn  
*Institute of Physics, Karl-Franzens-University, Universitätsplatz 5, 8010 Graz, Austria*

(Received 2 September 2014; accepted 16 October 2014; published online 29 October 2014)

The confinement of surface plasmon modes in flat nanoparticles gives rise to plasmonic breathing modes. With a vanishing net dipole moment, breathing modes do not radiate, i.e., they are optically dark. Having thus escaped optical detection, breathing modes were only recently revealed in silver nanodisks with electron energy loss spectroscopy in an electron microscope. We show that for disk diameters  $>200$  nm, retardation induced by oblique optical illumination relaxes the optically dark character. This makes breathing modes and thus the full plasmonic mode spectrum accessible to optical spectroscopy. The experimental spectroscopy data are in excellent agreement with numerical simulations. © 2014 AIP Publishing LLC. [<http://dx.doi.org/10.1063/1.4900615>]

Plasmonic nanoparticles made of metals such as silver, gold, or aluminum are prominent examples for strong light-matter interaction. The free metal electrons are driven to resonant oscillations at specific light frequencies that are set by the choice of the metal, the surrounding medium, and the particle geometry.<sup>1</sup> The resulting strong field enhancement and confinement plays an important role in surface enhanced spectroscopy,<sup>2</sup> nonlinear optics,<sup>3</sup> and near field microscopy<sup>4</sup> and it is exploited in applications such as data storage<sup>5</sup> or biosensing.<sup>6</sup> While spherical nanoparticles are well described by Mie theory, the plasmonic mode spectrum of (lithographically fabricated) flat nanoparticles, e.g., nanodisks, can be decomposed into film and edge modes.<sup>7</sup> On one hand, edge excitations constitute the well known dipole, quadrupole, and higher multipolar modes. On the other hand, the confinement by the particle boundaries transforms the film surface plasmon to radially symmetric “breathing” modes.<sup>8,9</sup> The fundamental breathing mode in a nanodisk is characterized by one circular and no radial node line, i.e., (0,1). This mode has thus a vanishing net dipole moment, i.e., it is optically dark (for disk diameters small compared to the light wavelength) and has thus escaped optical detection so far. It is, however, important to notice that dark modes can strongly interact with their immediate environment via their optical near field. This implies that dark modes can be probed by near field measurement schemes as provided, for example, by a passing electron beam, as recently employed to characterize breathing modes in silver nanodisks by electron energy loss spectroscopy in a transmission electron microscope.<sup>8</sup> It was shown that the optical mode density of breathing modes is particularly high, which emphasizes their importance for any kind of near field coupling, e.g., in the case of combining nanophotonic components or sensing schemes. It is thus of paramount importance to characterize (and tailor) the full mode spectrum of a plasmonic nanoparticle. In this letter, we aim at relaxing the dark character of the breathing modes in silver nanodisks by a proper choice of an oblique optical illumination geometry. We show that breathing modes can indeed be probed optically, thus making the full plasmonic mode spectrum of nanodisks accessible to

standard optical spectroscopy. We corroborate the experimental data with numerical simulations that show an excellent agreement.

Silver nanodisks are fabricated in regular square arrays (periodicity 1200 nm) by electron beam lithography using a poly(methyl methacrylate) resist on quartz substrates. Exposure and chemical development are followed by the evaporation of 30 nm mass thickness of silver and lift-off. The disk diameters are 115–315 nm ( $\pm 2$  nm), as measured using a scanning electron microscope. Optical spectroscopy is done with a standard optical microscope (objective 10 $\times$ , numerical aperture 0.25), equipped with a halogen lamp source, a fiber-coupled spectrometer, and sample holder that can be tilted. Optical spectra are acquired in transmission (transmittance  $T$ ), corrected to the instrument response ( $T_0$ ), and plotted as  $1 - T/T_0$ , as a measure of the fraction of the light that is absorbed and scattered by the nanoparticle array.

The optical spectra of 30 nm high silver nanodisks with diameters of 115–315 nm, as acquired in perpendicular incidence, are summarized in Fig. 1(a). For small diameters, the (in-plane) dipole ( $D$ ) excitation is the only peak in the spectra. This dipole peak shifts to longer wavelengths as the disk diameter is increased, as expected for an increasing particle axis ratio. For disks larger than 200 nm another peak appears close to the wavelength of 400 nm. The corresponding simulated spectra are plotted in Fig. 1(b). The simulations were performed with the MNPBEM toolbox<sup>10</sup> that relies on the boundary element method.<sup>11</sup> The permittivity of silver was taken from the tabulated data in Ref. 12, and the presence of the substrate was taken into account as an effective bulk index of 1.30 of the medium surrounding the particle. We calculate the extinction cross sections as a sum of the absorption and scattering cross sections,  $\sigma_{\text{ext}} = \sigma_{\text{abs}} + \sigma_{\text{sca}}$  for single nanoparticles, a value that can be directly compared to the experimental measurements on the nanodisk arrays. We find an excellent agreement of the simulated and the measured spectra. Plotting the corresponding charge distribution (inset in Fig. 1(b)) confirms the dominant peak as corresponding to the dipole excitation. The charge pattern of the short-wavelength peak shows that this excitation corresponds to the (1,1) disk mode,<sup>8,13</sup> which is of odd symmetry (giving rise to a net dipole moment) and thus coupling to light.

<sup>a)</sup>Electronic mail: markus.krug@uni-graz.at

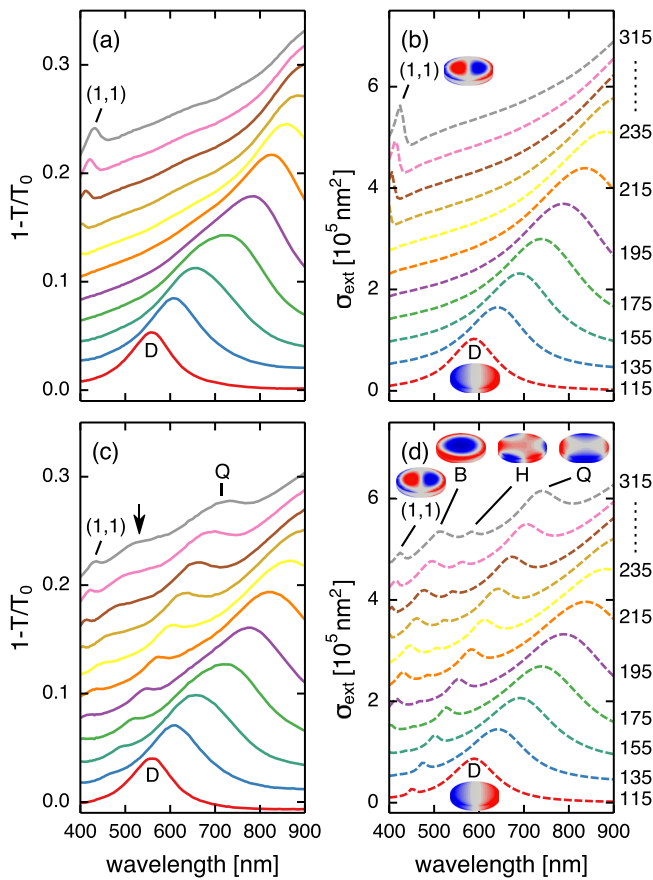


FIG. 1. Optical spectra of silver nanodisks with diameters of 115–315 nm (given by the numbers on the right side) and a height of 30 nm. (a) Experimental and (b) simulated spectra for perpendicular incidence, the insets depict the charge distribution of the dipole (D) and the (1,1) modes. (c) Experimental and (d) simulated spectra for an incidence angle of  $30^\circ$ , the inset depicts in addition the charge distribution of the quadrupole (Q), hexapole (H), and breathing (B) modes. The arrow in (c) marks the broad feature corresponding in spectral position to the B and H modes in (d). The spectra are offset for clarity.

We now turn to the analysis of the optical spectra acquired at oblique incidence. The rationale behind this approach is to introduce significant phase retardation across the nanodisk diameter to relax the symmetry condition that prevents the coupling of the breathing mode to light (compare the inset of Fig. 3(b)). Depending on incidence angle, light wavelength, and disk diameter, retardation can support the coupling of light and plasmonic modes that is “forbidden” for perpendicular incidence.<sup>14</sup> Fig. 1(c) shows the experimental spectra for the same samples as in Fig. 1(a), but now for an angle of incidence of  $30^\circ$ . Both the dipole and the (1,1) modes are reduced in intensity as compared to perpendicular incidence. This can be readily assigned to reduced excitation by light as only the electric field component parallel to the substrate plane can couple to these modes. Importantly, new peaks appear, in agreement with the simulations in Fig. 1(d). Again, plotting the charge patterns is helpful for identifying the modes. We find that the prominent peak labeled Q corresponds to the quadrupole mode, and that the two further modes found in the simulated spectra correspond to the hexapole (H) mode and indeed the breathing (B) mode. However, these two latter modes cannot be clearly identified in the experimental data in Fig. 1(c),

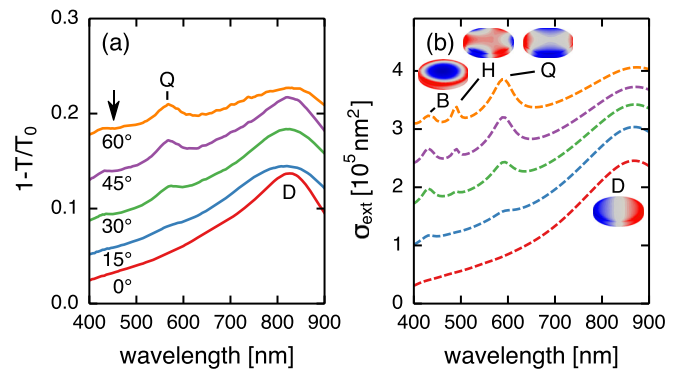


FIG. 2. Optical spectra of silver nanodisks with a diameter of 215 nm and a height of 30 nm. (a) Experimental and (b) simulated spectra for the given incidence angles. The insets depict the charge distributions of the dipole (D), quadrupole (Q), hexapole (H), and breathing (B) modes. The arrow in (a) marks the broad feature corresponding in spectral position to the B and H modes in (b). The spectra are offset for clarity.

where rather one broad feature in the relevant spectral range is observed.

We illustrate the role of the incidence angle for the array of nanodisks with diameters of 215 nm in Fig. 2(a). Clearly, the quadrupole peak emerges as a function of illumination angle, in accordance with the expected angular mode profile. In addition to the quadrupole peak, there is a broad feature marked by the arrow at lower wavelengths. In contrast to the simulated data in Fig. 2(b), the experiment again cannot spectrally resolve the hexapole and breathing modes. Besides the rather weak coupling efficiencies and thus spectral signal strengths, reasons therefore might include peak broadening due to inhomogeneous disk geometry variations within the array.

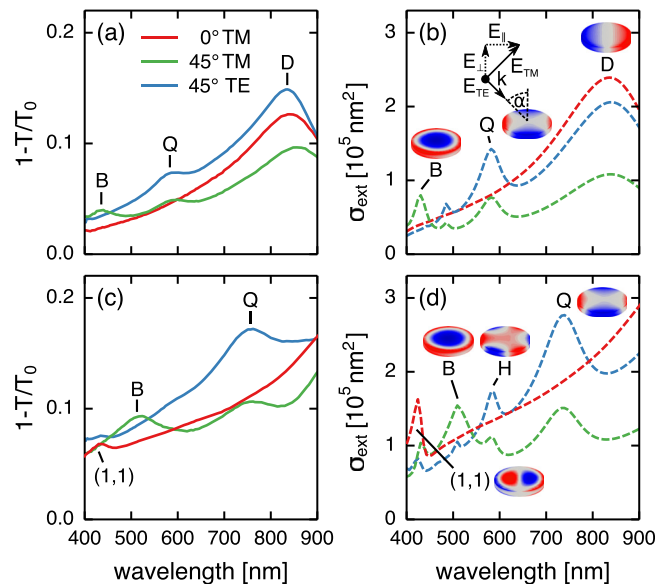


FIG. 3. Optical spectra of silver nanodisks with a height of 30 nm for an incidence angle of  $45^\circ$ . (a) Experimental and (b) simulated spectra for disks with a diameter of 215 nm. The inset in (b) sketches the polarization conditions for inclined incidence;  $k$  is the wavevector,  $E_{\text{TM}}$  (with components  $E_{\parallel}$  and  $E_{\perp}$ ) and  $E_{\text{TE}}$  are the electric field vectors for TM and TE polarization, respectively, and  $\alpha$  is the incidence angle. The insets in (b) depict the charge distributions of the dipole (D), quadrupole (Q), and breathing (B) modes. (c) and (d) same as (a) and (b), but for disks with a diameter of 315 nm.

To improve the experimental conditions, we consider the transverse magnetic (TM) character of (film) surface plasmons and thus of the breathing mode and include polarization control to our measurement. As suggested by the inset in Fig. 3(b), retardation is expected to give rise to a field distribution across the disk that for symmetry reasons couples to the breathing mode only for TM-polarization. We thus expect improved signal strength for the polarization-controlled spectra. Fig. 3(a) shows the experimental spectra acquired on an array of nanodisks 215 nm in diameter for an incidence angle of 45° for both TM-polarization (green) and TE-polarization (blue). For reference, the spectrum for perpendicular incidence (red) is also included. First, the dipole (D) and quadrupole (Q) peaks are significantly stronger for TE-polarization, as the full electric field contributes to the excitation of these in-plane modes. Second, the breathing mode (B) is now indeed clearly observable around a wavelength of 430 nm. With all peaks red-shifted and stronger B and Q peak strengths due to increased retardation, the same observations are made for disks with a diameter of 315 nm, Fig. 3(c). All experimental data agree qualitatively very well with the corresponding simulations depicted in Figs. 3(b) and 3(d). Furthermore, the results are in agreement with the mode symmetry found in circular plasmonic patch nanoantennas.<sup>15</sup> It is interesting to note that only disks with diameters > 200 nm yielded clearly identifiable breathing mode signatures, which we thus take as the onset of efficient retardation-induced coupling to these radial modes.

In summary, we have optically probed the plasmonic breathing modes of silver nanodisks by employing retardation induced by oblique light incidence. We have shown that for adequate particle diameters, standard optical spectroscopy can probe the full mode spectrum of plasmonic

nanoparticles. While not coupling to light in standard (perpendicular incidence) geometries, dark modes are important for nanophotonic architectures including plasmonic particles or, e.g., sensing due to their particularly strong near fields. Breathing modes have thus been taken into account and they should be accordingly characterized.

Financial support from the FWF SFB NextLite (F4905-N23, F4906-N23) and the FWF Project P24511-N26 was acknowledged.

<sup>1</sup>M. Pelton and G. Bryant, *Introduction to Metal-Nanoparticle Plasmonics* (John Wiley & Sons, New York, NY, 2013).

<sup>2</sup>E. C. L. Ru and P. G. Etchegoin, *Principles of Surface-Enhanced Raman Spectroscopy and Related Plasmonic Effects* (Elsevier, Amsterdam, 2009).

<sup>3</sup>M. Kauranen and A. V. Zayats, *Nat. Photonics* **6**, 737 (2012).

<sup>4</sup>L. Novotny and S. J. Stranick, *Annu. Rev. Phys. Chem.* **57**, 303 (2006).

<sup>5</sup>W. A. Challener, C. Peng, A. V. Itagi, D. Karns, W. Peng, Y. Peng, X. Yang, X. Zhu, N. J. Gokemeijer, Y. T. Hsia *et al.*, *Nat. Photonics* **3**, 220 (2009).

<sup>6</sup>J. N. Anker, W. P. Hall, O. Lyandres, N. C. Shah, J. Zhao, and R. P. Van Duyne, *Nat. Mater.* **7**, 442 (2008).

<sup>7</sup>F.-P. Schmidt, H. Ditlbacher, U. Hohenester, A. Hohenau, F. Hofer, and J. R. Krenn, *Nat. Commun.* **5**, 3604 (2014).

<sup>8</sup>F.-P. Schmidt, H. Ditlbacher, U. Hohenester, A. Hohenau, F. Hofer, and J. R. Krenn, *Nano Lett.* **12**, 5780 (2012).

<sup>9</sup>A. Chakrabarty, F. Wang, F. Minkowski, K. Sun, and Q.-H. Wei, *Opt. Express* **20**, 11615 (2012).

<sup>10</sup>U. Hohenester and A. Trügler, *Comput. Phys. Commun.* **183**, 370 (2012).

<sup>11</sup>F. de Abajo and A. Howie, *Phys. Revs. B* **65**, 115418 (2002).

<sup>12</sup>P. B. Johnson and R. W. Christy, *Phys. Rev. B* **6**, 4370 (1972).

<sup>13</sup>R. Filter, J. Qi, C. Rockstuhl, and F. Lederer, *Phys. Rev. B* **85**, 125429 (2012).

<sup>14</sup>G. Schider, J. R. Krenn, A. Hohenau, H. Ditlbacher, A. Leitner, F. R. Aussenegg, and W. L. Schaich, *Phys. Rev. B* **68**, 155427 (2003).

<sup>15</sup>F. Minkowski, F. Wang, A. Chakrabarty, and Q.-H. Wei, *Appl. Phys. Lett.* **104**, 021111 (2014).